

A Comparison of Lightning Flashes Observed by Ground-Based Detection Networks and Video

James J. Coy^{1,2}, and Kristin M. Calhoun^{3,4}

¹Research Experiences for Undergraduates, Norman, Oklahoma

²Texas A&M University, College Station, Texas

³Cooperative Institute for Mesoscale Meteorological Studies, University of Oklahoma, Norman, Oklahoma

⁴NOAA/National Severe Storms Laboratory, Norman, Oklahoma

ABSTRACT

Cloud-to-ground (CG) lightning flashes recorded by both the National Lightning Detection Network (NLDN) and Earth Networks Total Lightning Network (ENTLN) are compared with three-dimensional lightning mapping observations from the Oklahoma Lightning Mapping Array (OK-LMA) and storm chaser video recorded of the 31 May 2013 El Reno tornadic supercell. The El Reno Survey Project (El-Reno-Survey.net) was created to crowd-source the abundance of storm chaser video from this event and provide open-access to the scientific community of the data. An initial comparison of CG lightning flashes captured on these videos with CG data from NLDN revealed a disagreement on the total number of flashes, with NLDN recording many negative CG flashes at lower peak amplitude not apparent in any of the videos. For this study, the area of the comparison was expanded and data from both the ENTLN and LMA were used to compare the observations from each network in terms of timestamp, location detection, peak current, and polarity of each flash in the period 2230-2330 UTC. Initial results from the NLDN and ENTLN indicated a negative CG dominance, but, after a 15 kA peak current filter was applied, the NLDN indicated primarily positive CG polarity flashes while ENTLN still indicated primarily negative CG polarity. The average distance between the two networks for the same flash was more than 2 km and improved to approximately 1 km after the 15 kA filter was applied. When compared to video and the OK-LMA, both the NLDN and ENTLN had misclassifications of in-cloud (IC) lightning as CG flashes. Additionally, the charge analysis of OK-LMA revealed the NLDN-determined polarity as correct each time the NLDN and ENTLN disagreed. It is concluded that there is a major flaw in the ENTLN's ability to determine the polarity of CG flashes despite having roughly similar peak current magnitudes for most CG flash occurrences.

1. INTRODUCTION

Data provided by lightning detection networks have been utilized by researchers, forecasters, and the general public. Lightning data can provide insight into storm behavior as well as provide safety information for outdoor venues, and critical insight to private companies. Overall, individual that the data for lightning detection rely on them for providing accurate results.

A lightning flash is the result of transfer of charge between oppositely charged regions of a thunderstorm. These charge regions develop due to the charge created by collisions of ice crystals in the storm's updraft region often with large ice collecting one polarity and smaller ice another (Bruning et al. 2012). Flashes can be entirely in-cloud (IC) or come from cloud to ground (CG).

On 31 May 2013, a line of severe storms developed during the afternoon over

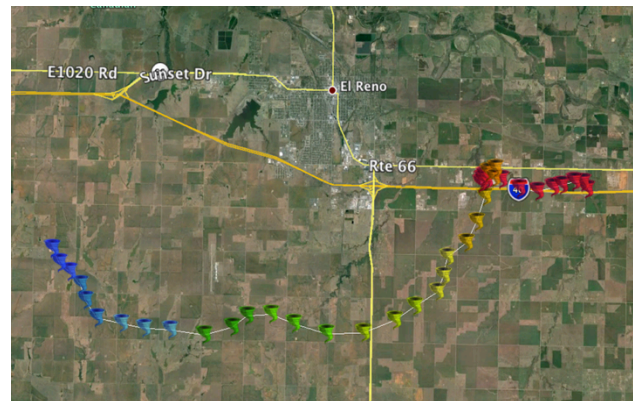


Figure 1. Google Earth image of the El Reno tornado path from 23:04:00 UTC to 23:42:00 UTC.

central Oklahoma in the United States (Lang et al. 2015). The strongest of these supercells produced a tornado (figure 1) lasting for about 40 minutes with a record-breaking peak width of about 2.6 miles and was eventually ranked an Enhanced Fujita scale 3 (EF3) near El Reno,

OK. Many storm chasers gathered around from all angles of the storm to record the event that had unfolded while unintentionally recording lightning flashes and cloud-to-ground (CG) strikes. Because of the great amount of video content, it prompted a team of scientists to create a website called the El-Reno-Survey.net to gather footage of the event from numerous storm chasers for scientific use (Seimon et al. 2014). In the initial study, they noticed that the National Lightning Detection Network recorded multiple CG flashes that were not visible on any of the chaser videos though their time and location matched. This analysis will further investigate this initial finding by comparing the NLDN and chaser videos with lightning detection data from other networks in order to discover and understand possible flaws and limitations of each.

2. DATA SOURCES

2.1 National Lightning Detection Network

The NLDN, operated by Vaisala Inc., has been operational since 1989 (Cummins and Murphy et al. 2009). Currently, the network consists of over 100 sensors roughly evenly distributed across the continental United States providing real-time and historical lightning data for researchers and industries (Cummins and Murphy et al. 2009). The network received major upgrades during 1994-1995, 2002-2003 (Cummins and Murphy et al. 2009), and 2013 (Murphy et al. 2014) with intentions of improved lightning detection efficiency. The 2002-2003 upgrade primarily dealt with the NLDN's ability to detect CG lightning. This upgrade allowed the NLDN to detect CG flashes with the minimum requirement of 2 sensors by modifying the sensors to detect large-amplitude very low frequency (VLF) and low frequency (LF) pulses in cloud flashes (Cummins and Murphy et al. 2009). Currently the NLDN has a CG flash detection efficiency of at least 95% with a median location accuracy of at most 200 meters (Lang et al. 2015). The timestamp, latitude/longitude, peak current, and polarity of the CG flashes recorded by the network was used for this analysis.

2.2 Earth Networks Total Lightning Network

The Earth Networks Total Lightning Network (ENTLN) was initially made operational in 2009 using a small set of sensors and then expanded throughout the continental United

States in 2010 (Thompson et al. 2014) with a lower concentration of sensors in the western mountainous regions. The network now consists of over 800 sensors in 40 countries around the world (ENTLN 2014). The ENTLN sensors use a wideband system with a lightning detection frequency ranging from 1 HZ to 12 MHZ. The wide frequency range of the sensors allows the network to not only detect CG flashes but also weak in-cloud (IC) pulses (Liu and Heckman et al. 2012). To distinguish between these types of flashes, those with at least 1 return stroke are classified as a CG flash (Thompson et al 2014). In order for a flash to be confirmed, a minimum of 5 sensors is required to record the occurrence (Thompson et al. 2014). Similar the NLDN, the ENTLN has a CG flash detection efficiency of 95% and a median location accuracy of at most 200 m in our region of study in central Oklahoma. The timestamp, latitude/longitude, peak current, and polarity of the CG flashes recorded by the network were used for this analysis.

2.3 Oklahoma Lightning Mapping Array

The Oklahoma Lightning Mapping Array (OK-LMA) produces 3-dimensional images of individual lightning discharges or the overall activity of storms by locating the sources of impulsive signals on the very high frequency (VHF) range (Krehbiel et al. 2002). The network consists of 12 stations concentrated in central Oklahoma measuring the time and signal amplitude of the largest signal radiated by lightning during each 80-100 μ s period (MacGorman et al. 2011). In order for a source to be recorded, a minimum of 6 stations must have observed it. Lightning is mapped with an accuracy of 50 meters but gradually has less accuracy going away, reducing to an accuracy of 2 km in the maximum recording range of 200 km (MacGorman et al. 2011). For the period of interest, the El Reno supercell was near the central range of the OK-LMA. In this analysis, the OK-LMA is used as "truth" for identifying that a flash occurred in the relative location and timestamp of the NLDN and ENTLN inferred CG occurrence. The OK-LMA will also be used to determine the polarity of CG flashes through charge analysis.

2.4 El-Reno-Survey.net Chaser Footage

The El-Reno-Survey.net website was created by David Hoadley, Dr. Tracie Seimon,

Dr. Anton Seimon, Dr. John Allen, and Elke Edwards. The website consists of crowdsourced video footage of the El Reno storm during its tornadic period. The purpose of gathering the footage was to allow for scientific use, such as providing a multi-perspective of storm and tornado evolution in comparison to dual-Doppler analysis. From this data, one hour of footage is used beginning at 22:30:00 UTC. All videos are rendered to play at 30 frames per second. The videos used in this study also include metadata that lists the latitude and longitude position of the chaser. The videos are considered ground truth in observing CG that a CG flash did occur.

3. METHODOLOGY

The time period chosen was during 22:30:00-23:30:00 UTC based on the provided footage, capturing the mesocyclone to when the tornado went along I-40 (as indicated on Fig. 1). An initial analysis of NLDN and video matched flashes was provided by Dr. Anton Seimon with each CG flash and video flash matched according to timestamp by the millisecond. The area of study for this analysis was expanded to incorporate the entire supercell storm, without including another strong cell closely northeast. Additionally, a 15 kA peak current filter was applied to the CG data inspired both by Cummins et al. 2006, who used a 10 kA filter

and Calhoun et al. 2014, who used a 15 kA filter for the analysis of another Oklahoma supercellular storm. This filter is designed to remove possible misclassified IC flashes as CG flashes and was applied to both the NLDN and ENTLN CG data.

Data from the OK-LMA were analyzed using the XLMA software (New Mexico Tech). Starting from the most intense peak current, each NLDN- and ENTLN- reported CG flash was isolated by timestamp and relative location. The VHF source points forming the structure of the flash are color by timestamp with blue representing the start of the flash and red representing the end. The observed charge structure and propagation of the flash determined whether it was CG or IC.

For the inferred charging regions, flashes are thought to be initiated in the transitional regions between positive and negative charge. After initiating, channel leaders of opposite polarity propagate in different directions from the location of initiation (Bruning et al. 2010). This is known as the bi-directional leader theory, which emphasizes that the essential factor in maintaining lightning discharge is the continuing breakdown at the tip of the positive, negative, or both ends of the lightning leader that extends the channel into new cloud regions with stored electrostatic energy (Mazur and Ruhnke et al. 1998).

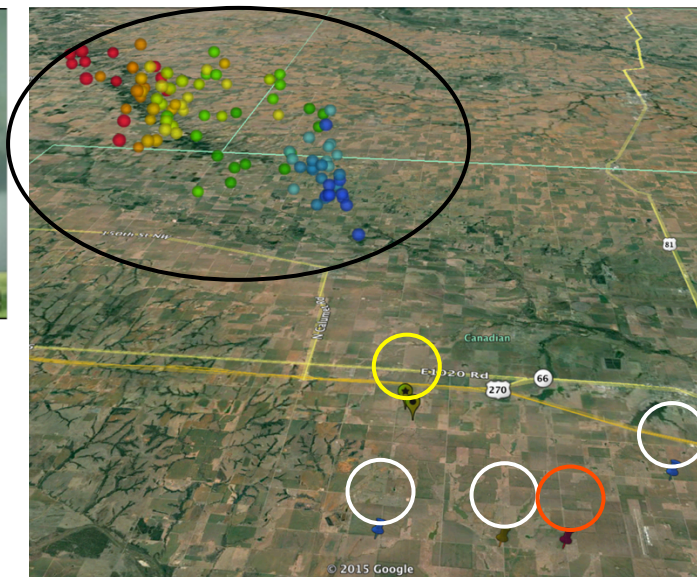
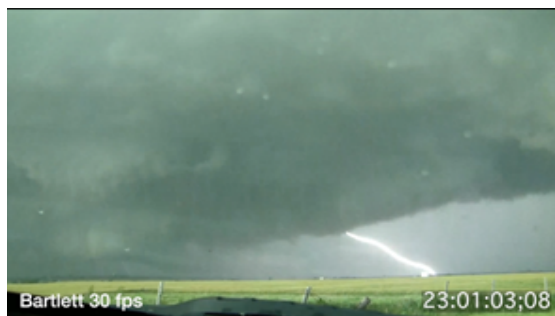


Figure 2. An example of a video (top) confirmed CG strike reported by all resources occurring at 23:01:03 UTC shown on Google Earth (right). The dots (circled black) colored by timestamp represents the OK-LMA mapping of the flash, the markers at ground-level (circled yellow) represents NLDN and ENTLN inferred location of the flash, and the pushpin markers (circled white) represents the location of the chasers who saw the strike. The pushpin circled red is the point of view of the video shown.

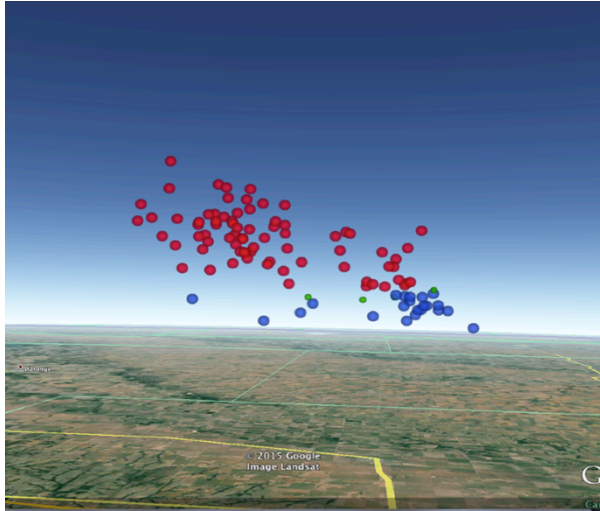


Figure 3. OK-LMA charge analysis output for the same CG flash shown on figure 2. Red dots represents the positive region of the storm and the blue dots represent the negative region of the storm.

Negative leaders propagate more impulsively, and thus produce more VHF source than positive leaders (Bruning et al. 2010). For the detection of CG flashes through the OK-LMA, negative CGs (-CG) will be typically clearly visible while positive CGs (+CG) will be harder to identify. The XLMA was used to complete the charge analysis subjectively, manually labeling the source points as blue (negative charge), red (positive charge), or green (undetermined charge).

For the video analysis, each observed flash (regardless of it being CG) was recorded in the metadata provided by the chaser. The chasers also recorded the GPS position which made it possible to create a path of each chaser on Google Earth. Various roads and landmarks such as hotels or restaurants were also used to determine the relative location of a flash that was observed. Flashes from video were suspected of being CG by either viewing an actual bolt from cloud to ground or by timestamp and location from the networks if only a flash of light was seen. The frame counter on each video made it possible to convert it to milliseconds in order for the flash to be accurately matched to the NLDN, ENTLN,

and/or OK-LMA data.

After the CG flashes were matched in time and space, they were plotted on Google Earth to create a 3-dimensional perspective of each CG flash occurrence (Figure 2). Charge analysis of each flash done on the XLMA was also displayed on Google Earth (Figure 3) and polarity between the NLDN, ENTLN, and OK-LMA were compared. Additionally, the locations and peak currents of each flash were compared between the NLDN and ENTLN.

4. RESULTS

4.1 *EI-Reno-Survey.net's* NLDN and Video Pre-analysis Results

NLDN CG Flashes	# NLDN and Video Strike	# NLDN and Video Flash	Video Only	% +CG
237	102	91	13	98%

Table 1. NLDN and Video analysis results done by the team of the EI-Reno-Survey.net.

The initial comparison of NLDN and chaser videos by Anton et al. 2014 had a total of 237 CG flashes recorded with 193 of the 237 seen on video (Table 1). Of the total NLDN recorded flashes, 98% of them were determined to be +CG which implies that the mesocyclone region of the storm during this time had predominately +CG flashes. The analysis for this project began with initial comparison, but the following sections will expand on the region of interest to the entire supercell storm and add data from the ENTLN and the OK-LMA.

4.2 NLDN and ENTLN Comparison Results

NLDN CG Flashes	ENTLN CG Flashes	Total CG Flashes	NLDN/ENTLN
2117	1672	3232	557
1682 (15 kA filter)	1113 (15 kA filter)		264 (15 kA filter)

Table 2. Overall NLDN and ENTLN reported CG flashes during 22:30:00 UTC through 23:30:00 UTC.

NLDN % -CG	NLDN % +CG	ENTLN % -CG	ENTLN % +CG	% Agreed Polarity	Avg. Distance Agreement (m)
58%	42%	77%	23%	72%	2321
16% (15 kA filter)	84% (15 kA filter)	63% (15 kA filter)	37% (15 kA filter)	53% (15 kA filter)	1232 (15 kA filter)

Table 3. Statistics of the 557 NLDN and ENTLN matched CG flashes (2nd row) and with 264 CG flashes of the 15 kA filter (3rd row).

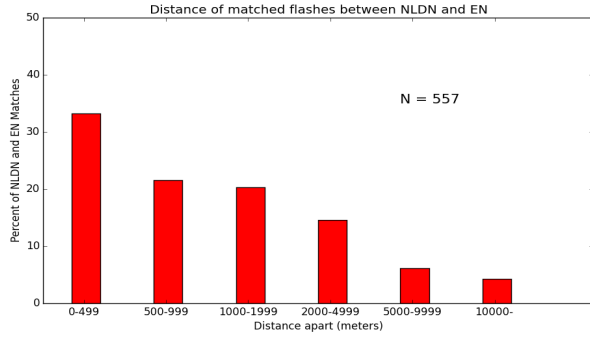


Figure 4. NLDN and ENLTLN distance agreement chart. Percentage of the 557 matched flashes into distance intervals.

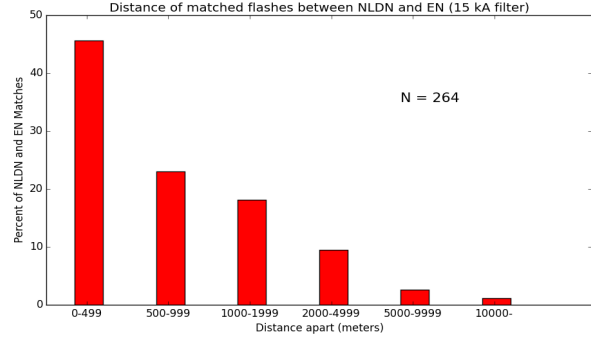


Figure 5. NLDN and ENLTLN distance agreement chart. Percentage of the 264 matched flashes into distance intervals with a 15 kA filter.

A total of 3232 individual CG flashes were recorded by both NLDN and ENLTLN during the one hour period (Table 2). Of those, NLDN recorded 2117 CG flashes while ENLTLN recorded 1672 CG flashes. 557 of the 3232 flashes were matched by the NLDN and ENLTLN using a timestamp difference of at most 10 milliseconds. After the 15 kA filter was applied, the number of NLDN CG flashes reduced by approximately 20% to 1682 and ENLTLN CG flashes to about a 35% decrease to 1113. The 15 kA filter is appropriate, as only 3 of the NLDN and/or ENLTLN recorded CG flashes whose peak currents were below 15 kA were seen on video and/or the OK-LMA as a ground flash. After the 15 kA filter, the number of NLDN and ENLTLN matched flashes reduced to 264 from 557 (roughly 50%).

that one of the networks could be erroneous in determining the polarity of CG flashes. The application of the filter improves the average distance agreement but worsens the polarity agreement between the NLDN and ENLTLN (Table 3).

Focusing the analysis to the 264 matched CG flashes, table 3 shows polarity percentages and average distance agreements between the two networks. During the one hour period of the study, with the 15 kA filter, NLDN indicates that the storm was predominately +CG while ENLTLN stays indicating that the storm was predominately -CG. Overall, their agreed polarity reduced from 72% to 53%. This reveals

For the distance agreement analysis, Fig. 4 shows the percentage of the 557 NLDN and ENLTLN matched CG flashes sorted into distance intervals. Fig 5 shows the same comparison with a 15 kA filter applied. Nearly 70% of the 264 matched flashes have inferred location distances between 0-1 km. Outliers, went slightly down with inferred location distances greater than 10000 km became nearly nonexistent compared to Fig. 4. This indicates that the filter removed CG flashes that were most likely had one of the networks correctly locate it. IC flashes do propagate both horizontally and vertically and it is possible for the NLDN to record a part of the flash while the ENLTLN records a different part of the flash further away.

For the peak current difference analysis, Fig. 6 shows the distribution of matched flashes according to their difference intervals ignoring polarity. Fig. 7 shows the same peak current

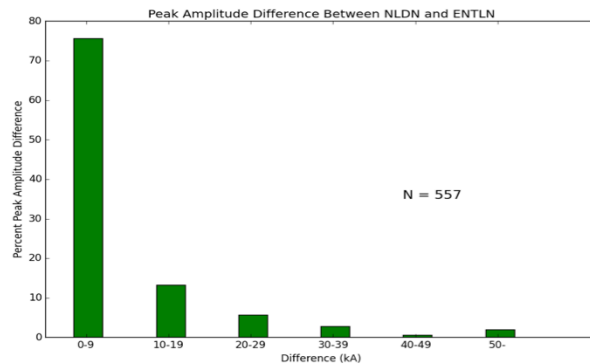


Figure 6. Peak current comparison chart between the NLDN and ENLTLN. Percentages of matched flashes are separated into peak current difference intervals by the kA.

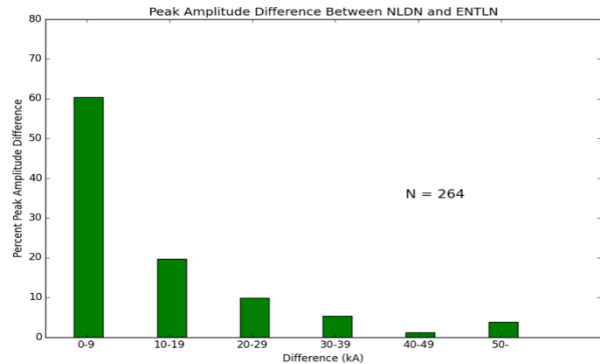


Figure 7. Peak current comparison chart between the NLDN and ENLTLN with the 15 kA filter applied. Percentages of matched flashes are separated into peak

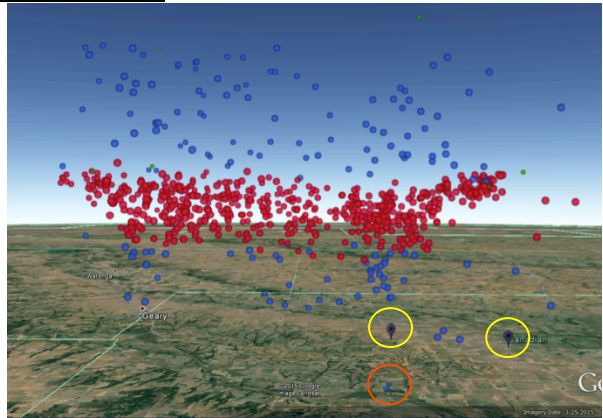
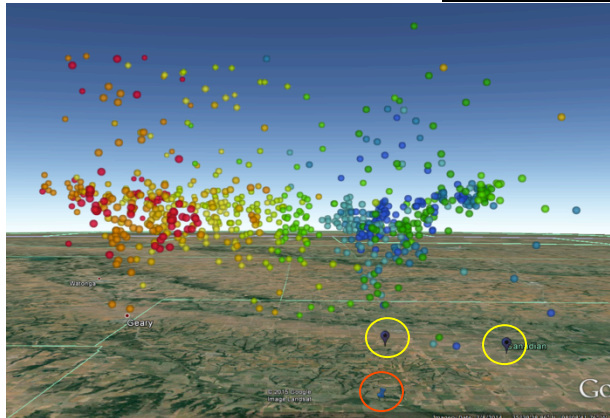


Figure 9. A video confirmed (top middle) CG strike occurring at 22:32:21 UTC with NLDN (circled yellow), ENTLN (circled yellow), and OK-LMA recorded data (right). Through charge analysis (left), the OK-LMA inferred polarity of the strike was +CG with NLDN and ENTLN all agreeing on the polarity as well. The position that the video was recording is circled red.

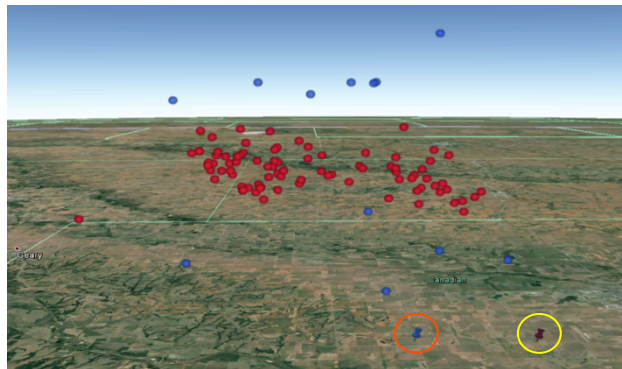
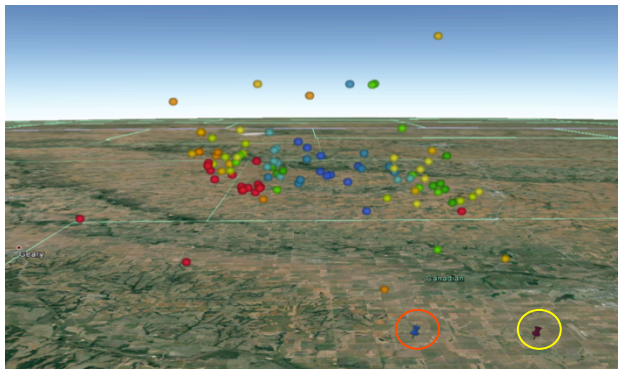


Figure 9. A video confirmed (top middle) CG strike occurring at 22:59:06 UTC with OK-LMA recorded data only (right). Through charge analysis (left), the OK-LMA inferred polarity of the strike was +CG. The position that the video was recording is circled red.

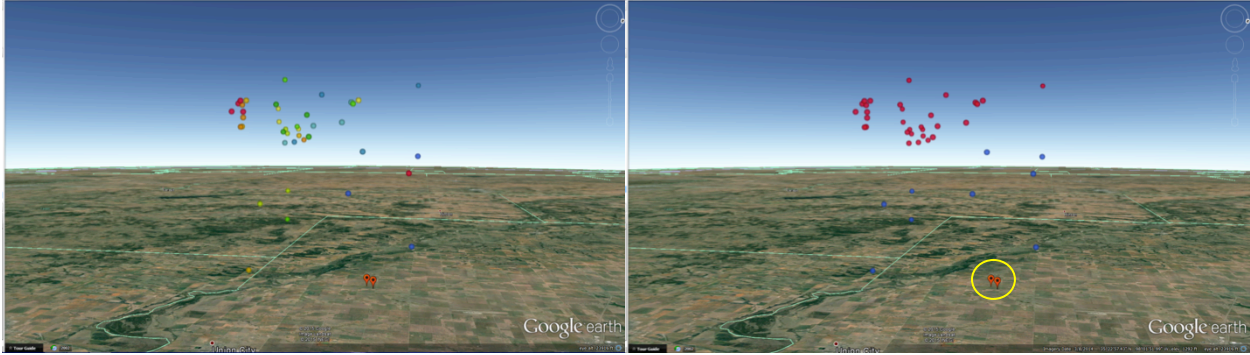


Figure 11. An NLDN, ENTLN (circled yellow), and OK-LMA recorded CG flash that occurred at 23:13:30 UTC (left) with the most powerful peak current of 247 kA (NLDN). NLDN and the OK-LMA, through charge analysis (right), indicates a +CG while ENTLN indicates a -CG

differences between 0-9 kA went from representing over 70% of the 557 matched flashes to 60% of the 264 filtered matched flashes.

4.3 NLDN, ENTLN, OK-LMA, and Video Comparison Results

4.3a Individual Results

Not every video confirmed CG strike or NLDN and ENTLN recorded CG flash had the same results. Some CG flashes were recorded by only NLDN or ENTLN and some that were video confirmed were not recorded by either.

Fig. 9 shows a video confirmed CG strike occurring at 22:32:21 UTC plotted on Google Earth. The strike was unanimously determined by the NLDN, ENTLN, and the OK-LMA to have a positive polarity. The flash was rather complex based on the OK-LMA data allowing the observance of a 3-layered charge structure with the lowest and highest regions being negative and middle region being positive.

Fig. 10 shows a video confirmed CG strike occurring at 22:59:06 UTC with the OK-LMA data plotted. Through charge analysis,

this strike was inferred to have a positive polarity. This CG strike was surprisingly not recorded by either NLDN or ENTLN.

Fig. 11 shows an NLDN, ENTLN, and OK-LMA plotted CG flash occurring at 23:13:30 UTC. Though not video confirmed, this flash had the highest peak current observed by both NLDN (247 kA) and ENTLN (224 kA). However, the NLDN recorded the CG flash as being positive while the ENTLN recorded it as being negative. Through charge analysis, the OK-LMA inferred charge was positive. This indicates that the ENTLN recorded the wrong polarity of the flash along despite the magnitude of the peak current was close to that of the NLDN's.

4.3b Overall Results

Five videos from storm chasers were fully analyzed for the one hour period of the analysis. These videos recorded 170 flashes with direct evidence of CG connection for 18 flashes (Table 4). The flashes were then matched to the NLDN and ENTLN data included with 29 other high amplitude flashes from the storm, but were not in the angle of viewing for the videos for charge analysis using the LMA.

LMA Analyzed CG Flashes	# Misclassified ICs	LMA Inferred +CG	# NLDN CGs	NLDN % +CG	# ENTLN CGs	ENTLN % +CG
199	2	100%	178	96%	175	48%

Observed Video Flashes	Other High Amplitude (kA) Flashes
170	29

Table 4. A set of tables showing the amount of video, OK-LMA, NLDN, and ENTLN reported flashes and their polarity statistics used in the full analysis.

Of these 199 flashes, 178 were recorded by NLDN and 175 were recorded by ENTLN as CG flashes. There were only 2 IC flashes that were misclassified as they showed no relative propagation toward the ground according to the OK-LMA. According to the charge analysis we infer that all of these 197 flashes were positive polarity. NLDN recorded 96% of these as +CG but only 48% were reported to be +CG by ENTLN. This points to a likely polarity inaccuracy in the ENTLN data. The use of the 15 kA filter, meanwhile, appears to remove a majority of the misclassified –CG flashes from the data set.

5. DISCUSSION

5.1 Videos and the CG Detection Networks

In this analysis, only 18 flashes were confirmed on video to have visible channels to ground. NLDN and/or ENTLN recorded 17 of those flashes. The conclusion of which network was the most accurate by inferred location remains questionable. A study done by Warner et al. 2013, did a similar comparison with confirmed upward CG flashes initiated by towers using video and only NLDN data. Since the towers are clearly seen in the video, the location of each recorded CG strike was always known. This allowed Warner to determine the true accuracy of the NLDN. For this analysis, however, the video confirmed CG strikes always occurred at a far enough distance where their location could not be found with certainty. Due to time constraints, we could not triangulate the location though it would be possible using trigonometry. Even though the OK-LMA was the most accurate among the NLDN and ENTLN, it was uncertain where exactly the strike occurred since they were all +CGs.

5.2 A Flaw in the ENTLN

It seems that the NLDN and ENTLN have difficulty in identifying –CG flashes as most of them recorded were of low peak current so they were easily filtered out and were not recorded on video. Interestingly, for +CGs, NLDN had its lowest peak current at 15 kA which prompted the creation of the 15 kA filter and not the 10 kA filter from Cummins' previous studies. Since the NLDN detects CG flashes by observing large amplitude VLF to LF pulses, it would most likely lead the network to more accurately detect +CG flashes than –CGs as +CGs emit VLF pulses (Jacobson et al. 1999).

The change of NLDN's implied dominance of CG polarity (table 3) shows how much of a difference it makes when a peak current filter is applied.

From the NLDN and ENTLN comparison to the comparison involving all resources, the ENTLN strongly disagrees with the inferred polarity of the NLDN and OK-LMA. Even with the 15 kA filter, there is further disagreement of polarity. Even though this was prevalent, most of the NLDN and ENTLN matched flashes did not have drastically different peak current regardless of polarity. After the 15 kA filter, however, the percentage of the most similar peak currents went down by more than 10%. This was unexpected as the purpose of the filter was to improve the similarities that the NLDN and ENTLN had recorded overall. Perhaps ENTLN's wideband frequency detection system causes the network to inaccurately determine the polarity of certain CG flashes since –CGs emit higher frequency radio waves than +CGs (Jacobson et al. 1999).

6. CONCLUSION

The NLDN, ENTLN, OK-LMA, and chaser videos were all compared based on recorded CG flashes during 22:30:00-23:30:00 UTC over a region concentrated near the rotation of the supercell and the tornado. ENTLN has a major flaw of determining the polarity of a CG flash. This can cause a possible researcher using the data provided by the network to become confused in trying to infer a net charge of the storm though CGs only make up a portion of the decision. Since during the time the cyclonic region of the storm was +CG dominant, this leads to limited performance of the NLDN, ENTLN, and OK-LMA. A more extensive study involving the entire supercell and a timeframe allowing to observe the storm's evolution would make it possible to study the networks' performance in detecting –CG lightning while still being cautious of low peak current flashes.

7. ACKNOWLEDGEMENTS

We would like to thank Dr. Anton Seimon for providing us with the chaser video footage and initial findings in order for this project to be made possible.

The corresponding author would like to thank his mentor Dr. Kristin Calhoun for her assistance throughout the term of the project and internship. Another thank you to Daphne

LaDue for selecting him to participate in the Research Experience for Undergraduates at the National Weather Center in Norman, Oklahoma.

This research was supported by National Science Foundation Grant (NSF) AGS-1062932. Funding was also provided by NOAA/Office of Oceanic and Atmospheric Research under NOAA–University of Oklahoma Cooperative Agreement NA11OAR4320072, U.S. Department of Commerce.

8. REFERENCES

Bruning, E. C., D. Rust, D. R. MacGorman, M. I. Biggerstaff, and T. J. Schuur., (2010): Formation of Charge Structures in a Supercell. *Monthly Weather Review.*, **138**, 3740-3761.

Cummins, K. L., M. J. Murphy., (2009): An Overview of Lightning Locating Systems: History, Techniques, and Data Uses, With an In-Depth Look at the U.S. NLDN. *IEEE Transactions on Electromagnetic Compatibility*, **51**, 3, 499-518, doi: 10.1109/TEMC.2009.2023450.

Jacobson, A. R., K. L. Cummins, M. Carter, P. Klingner, D. Roussel-Dupré, S. O. Knox., (1999): FORTE observations of lightning radio-frequency signatures: Prompt coincidence with strokes detected by the National Lightning Detection Network. *Radio-frequency Observations.*, 1-36.

Krehbiel, P., T. Hamlin, Y. Zhang, J. Harlin, R. Thomas, W. Rison., (2002): Three-Dimensional Total Lightning Observations with the Lightning Mapping Array. *2002 International Lightning Detection Conf.* 16-18 Oct 2002. Tucson, AZ.

Lang, T. J., S. A. Cummer, D. Petersen, L. Flores-Rivera, W. A. Lyons, D. R. MacGorman, W. Beasley., (2015), Large charge moment change lightning on 31 May to 1 June 2013, including the El Reno tornadic storm. *Geophys. Res. Atmos.*, **120**, 3354-3369, doi: 10.1002/2014JD022600.

Liu, C., S. Heckman., (2012): Total Lightning Data and Real-Time Severe Storm Prediction. *World Meteorological Organization.*, 1-12.

MacGorman, D. R., I. R. Apostolakopoulos, N. R. Lund, N. W. S. Demetriades, M. J. Murphy, P. R. Krehbiel., (2011): The Timing of Cloud-to-Ground Lightning Relative to Total Lightning Activity. *Monthly Weather Review.*, **139**, 3871-3886.

Mazur, V., L. H. Ruhnke., (1998): Model of electric charges in thunderstorms and associated lightning. *Journal of Geophysical Research.*, **103**, D18, 23299-23308.

Murphy, M. J., A. Nag, J. A. Cramer, A. E. Pifer., (2014): Enhanced cloud lightning performance of the U.S. National Lightning Detection Network following the 2013 upgrade. *23rd International Lightning Detection Conference.* 18-19 Mar 2014. Tucson, AZ.

OUN Webmaster, (2015): May 31-June 1, 2013 Tornado and Flash Flood Event. *National Weather Service Weather Forecast Office.* [Available online at: <http://www.srh.noaa.gov/oun/?n=events-20130531-elreno>].

Seimon, A., J. T. Allen, T. Seimon, E. Edwards, S. Talbot, and D. Hoadley, (2014): The El Reno Survey Project: Crowd-Sourced Database Development, Synchronous Photogrammetric Observations and 3-D Mapping of the Largest Documented Tornado. *27th Conf. on Severe Local Storms. Amer. Meteor. Soc.* 2-7 Nov 2014. Madison, WI. 13.5 [Available online at <https://ams.confex.com/ams/27SLS/webprogram/Paper254094.html>].

Thompson, K. B., M. G. Bateman, L. D. Carey., (2014): A Comparison of Two Ground-Based Lightning Detection Networks against the Satellite-Based Lightning Imaging Sensor (LIS). *Journal of Atmospheric and Oceanic Technology.* *Amer. Meteor. Soc.*, **31**, 2191-2205, doi: 10.1175/JTECH-D-13-00186.1. [Available online at: <http://journals.ametsoc.org/doi/pdf/10.1175/JTECH-D-13-00186.1>]